Antarctic bottom water flow through the Vema fracture zone

A. Vangriesheim
Centre Océanologique de Bretagne, BP 337, 29273 Brest Cedex, France.

ABSTRACT

During the October-November 1977 R/V "Jean Charcot" cruise, bathymetric and hydrological surveys of the Eastern Vema Fracture Zone were carried out in order to moor current meters on the sill located in the area, with the aim of evaluating the bottom water flow through this passage in the Mid-Atlantic Ridge. The sill zone in fact comprises a succession of three secondary sills situated between 40°52′W and 41°02′W at about 10°48′N, at depths ranging from 4 600 to 4 700 m.
Westward of the sills, there is a thick (750-950 m) bottom water layer of Antarctic origin. The potential temperature found at the bottom is 1.30°C. In the sill zone, the homogeneous layer is thinner and has a potential temperature of 1.40°C. Eastward of the sills, the homogeneous layer is 1 000 m thick, with $\Theta \sim 1.51$°C.
Five current meter moorings were deployed in this bottom layer: one was placed directly on the sills, one slightly to the east, two slightly to the west and the fifth 200 km further west.
Current speeds increase from west to east. Mean speeds range from ~ 3 cm/sec. at the western moorings to ~ 9 cm/sec. on the sills, reaching 25 cm/sec. at the eastern mooring, where the maximum speed was found to be 42 cm/sec. On and eastward of the sills, the current direction fluctuates slightly between east and north-east. These results confirm the eastward flow of Antarctic bottom water with a strong intensification above the sills.

Oceanol. Acta, 1980, **3**, 2, 199-207.

RÉSUMÉ

Passage d'eau de fond antarctique à travers la zone de fracture Vema

Au cours de la campagne du NO « Jean Charcot » en octobre-novembre 1977, une reconnaissance bathymétrique et hydrologique dans l'est de la zone de fracture Vema a été effectuée dans le but de mouiller des courantomètres autour du seuil situé dans cette zone, afin d'évaluer le passage d'eau de fond à travers ce passage dans la dorsale médio-atlantique. Ce seuil est en fait une succession de trois seuils secondaires entre 40°52′W et 41°02′W à environ 10°48′N à des profondeurs de 4 600 à 4 700 m.
A l'ouest des seuils, on trouve une couche d'eau de fond d'origine antarctique de 750 à 950 m d'épaisseur, avec une température potentielle sur le fond de 1,30°C. Sur la zone des seuils, la couche homogène est moins épaisse et la température potentielle est 1,40°C. A l'Est des seuils, la couche de fond a 1 000 m d'épaisseur, avec $\Theta \sim 1,51$°C.
Cinq lignes de courantomètres ont été mouillées dans cette couche d'eau de fond : une sur les seuils, une juste à l'Est, deux juste à l'Ouest et la dernière à 200 km à l'Ouest. Les vitesses mesurées augmentent d'Ouest en Est. Les vitesses moyennes sont ~ 3 cm/s à l'Ouest, ~ 9 cm/s sur le seuil et atteignent 25 cm/s à l'Est du seuil où la vitesse maximum est 42 cm/s. Sur le seuil et à l'Est du seuil, les directions du courant varient peu entre l'Est et le Nord-Est. Ces résultats confirment le passage vers l'Est d'eau de fond antarctique avec intensification de l'écoulement au niveau des seuils.

Oceanol. Acta, 1980, **3**, 2, 199-207.

INTRODUCTION

Deep circulation in the Atlantic Ocean is dominated by the northward spreading of Antarctic Bottom Water formed in the Antarctic Ocean. Above this bottom layer, North Atlantic Deep water flows toward the South Atlantic. The Antarctic Bottom Water spreads essentially west of the Mid-Atlantic Ridge, because the Walvis Ridge impedes its flow towards the eastern basins. Only a few deep passages in the Mid-Atlantic Ridge, including the Romanche Fracture Zone, the Vema Fracture Zone, etc., allow Antarctic Bottom Water to the reach eastern basins (see Fig. 1).

Further information was necessary in order to determine the precise bathymetry over the sill, to obtain hydrological and current measurements to describe the Antarctic Bottom Water flow through the Vema Fracture Zone, particularly over the sill, and to attempt to evaluate the volume transport.

The results presented here have been collected during the geological, geophysical and biological cruises which took place from October 11 to November 30, 1977 in the Vema Fracture Zone aboard the French R/V "Jean Charcot" with scientists from CNEXO-COB (Centre National pour l'Exploitation des Océans, Centre Océanologique de Bretagne). During these cruises, a
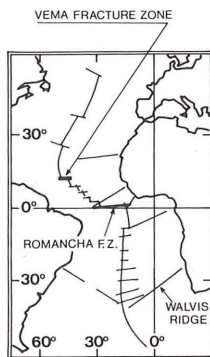

Figure 1

Vema fracture Zone localization in the Atlantic Ocean and its bathymetry (from Van Andel et al., 1971).

Position de la zone de fracture Vema dans l'Océan Atlantique et sa bathymétrie (d'après Van Andel *et al.*, 1971).

bathymetric survey, five hydrological stations were made and five current meter moorings were installed in the eastern part of the Fracture Zone. Their locations are listed in Table 1.
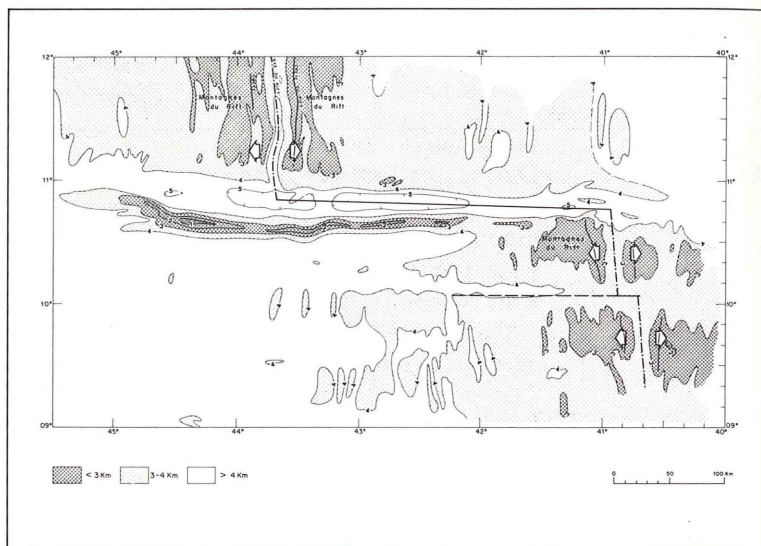
METHODS

Bathymetry

The Vema Fracture Zone, which links the Demerara abyssal plain to the Gambia abyssal plain, is a deep and narrow passage, oriented east-west, which transects the Mid-Atlantic ridge at about 11°N, offsetting it by more than 300 km between about 43°40'W and 41°W (see Fig. 1). Its location and depth allow it to play an important role in the process of bottom water circulation.

Previous studies have described this area, including those of Heezen *et al.* (1964), Van Andel *et al.* (1967) and then Van Andel *et al.* (1971). These show that the Vema Fracture Valley has a flat floor with depths of 5 200-5 300 m. The sediments, comprising turbidites from the Amazon, are more than 900 m thick. The width of this valley ranges between 8 and 20 km, except at its eastern end where it terminates at a sill. The hydrological findings of Heezen *et al.* (1964) suggest that the sill could be less than 4 500 m and lies between 40°30'W and 41°20'W.

A Lamont Cruise (Eittreim and Amos, 1974) found the expected sill at 4 840 m. The few hydrological data indicated a mixed bottom layer in the trough, the thickness of which increases from west to east, reaching 700 m just west of the sill.

The R/V "Jean Charcot" is equipped with the "Seabeam" (Renard, Allenou, 1979) multi-narrow beam echo sounder, which covers a width equal to 3/4 of the depth and gives a real time countour plotting at sea. A survey in the presumed area of the sill showed that the zone, in fact comprises a succession of 3 sills situated over a total distance of 17 km (Needham, pers. comm.). These are located at 41°01'W, 40°55'W and 40°53'W, with minimum depths of 4670 ± 10 m, 4630 ± 10 m and 4690 ± 10 m respectively (all depths in this paper are calculated with a sound velocity of 1 500 m/sec.). Figure 2 shows a bathymetric detail of the sill zone. In the following text, the set of three sills will be called "the sill".

On the south wall of the valley exists a transversal ridge with mean depths of 2 500 to 3 000 m, rising to 500 m. Another valley, south of this wall, reaches depths of 5 400 m, but its eastern end appears to be closed. In the following text, only the main valley, which is situated

Table 1
Locations and depths of CTD stations.
Locations and depths of current meter moorings.
Positions et profondeurs des stations CTD.
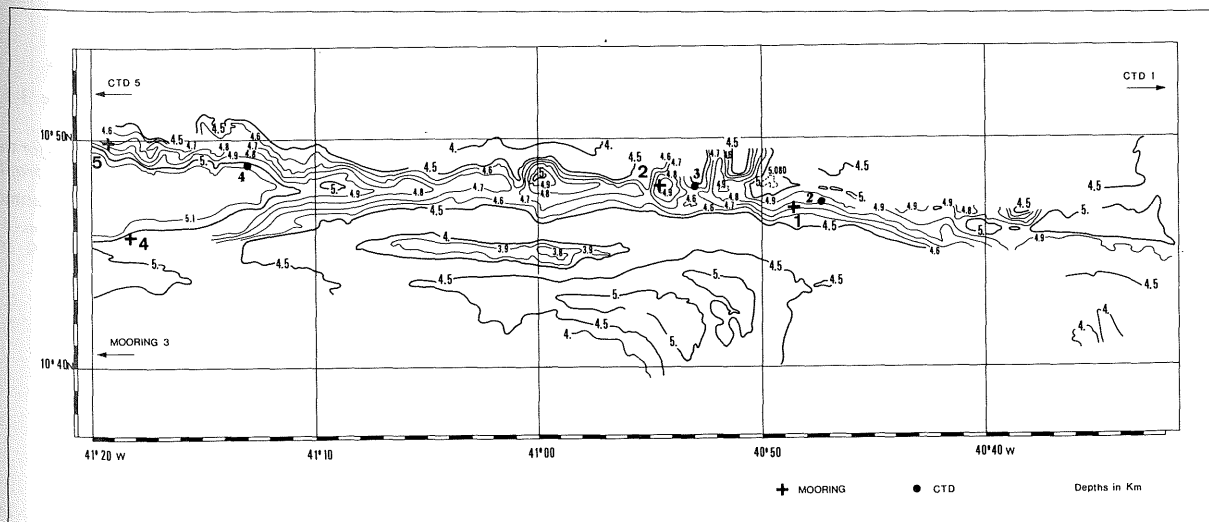Positions et profondeurs des mouillages de courantomètres.

Station CTD Nos.	Date	Location		Bottom depth (m)	Maximum depth Reached (m)
		Latitude	Longitude		
1	18 October 1977	10°44'2N	40°02'8W	5 400	5 452
2	19 October 1977	10°47'3N	40°47'3W	4 971	4 980
3	20 October 1977	10°47'9N	40°53'0W	4 920	4 944
4	20 October 1977	10°49'0N	41°13'0W	5 140	5 149
5	21 November 1977	10°46'3N	42°39'6W	5 150	5 166

	Theoretical depth (m)	Measured depth (m)	Record duration (day)
Mooring 1 : 10°47'N, 40°48'6W Bottom-depth: 4 960 m			
Mooring, 20 October 1977	4 650	4 520 to 4 429	33
Recovery, 22 November 1977	4 850	4 904	1.
	4 950	4 975	7.7
Mooring 2: 10°47'9N, 40°54'5W Bottom-depth: 4 920 m			
Mooring, 20 October 1977 Recovery, 22 November 1977	4 910	4 920	18
Mooring 3: 10°40'7N, 42°40'4W Bottom-depth: 3 998 m			
Mooring, 21 October 1977 Recovery, 21 November 1977	3 770	3 933 to 3 896	29.3
Mooring 4: 10°45'8N, 41°18'2W Bottom-depth: 5 000 m			
Mooring, 26 October 1977 Recovery, 22 November 1977	4 990	5 040	26
Mooring 5: 10°49'9N, 41°19'2W Bottom-depth: 4 950 m			
Mooring, 26 October 1977 Recovery, 22 November 1977	4 940	5 032	8.5

Figure 2

Bathymetric map of the sill area of the Vema Fracture Zone, showing positions of CTD stations and current meter moorings (Bathymetry from unpublished chart, D. Needham, pers. comm.).

Carte bathymétrique de la région du seuil de la zone de fracture Vema montrant les positions des profils CTD et des mouillages courantométriques (d'après document non publié, communication personnelle de D. Needham).

directly on the Fracture Zone axis will be considered, and will be called "the valley".

Hydrological measurements

In order to determine the deep hydrological structure west and east of the sill, a longitudinal section was carried out along the Vema Fracture valley. Five hydrological stations were made (see Fig. 2): the first at the eastern edge of the sill, at a depth of 5 400 m; the second just east of the sill; station No. 3 directy on the sill; station No. 4 at the entrance of the valley west of the sill; and station No. 5, 200 km further west, at the mid-point of the valley.

The Bissett-Berman CTD probe was equipped with an acoustic pinger to allow records as close as 1 m above the bottom. The temperature accuracy was 0.01°C, the salinity accuracy 0.02°/₀₀ and the depth accuracy 6 m.

Current measurements

Five moorings, equipped with Aanderaa RCM 5 and with AMF releases, were deployed on each side of the sill. The current meters could not be placed more than 5 000 m deep because of their container specifications. For each current meter, the conductivity channel was used to record a high resolution temperature signal between -2 and $+5$°C. The resolution obtained in this manner was 0.008°C.

Mooring 1, just east of the sill near station 2 (see Fig. 2), had three current meters at 10, 110 and 310 m above the bottom. Mooring 2 was just above the sill near station 3, with a single current meter 10 m above the bottom. Moorings 4 and 5, situated just west of the sill near station 4 on each side of the valley, just above the 5 000 m depth, were both equipped with a single current meter, 10 m above the bottom. Mooring 3, 200 km further west (near station 5) on the south flank of the valley, had a single current meter 230 m above the bottom.

All moorings were recovered but a certain amount of water penetrated five of the current meters at different times during the recording period. The data return is only 58%, with time-lengths varying from 1 to 33 days. The sampling interval was 5 minutes.

For the interpretation of data, it should be borne in mind that the results are not entirely homogeneous, due to the very different recording time-lengths and because the choice of mooring locations was limited by the pressure case specifications of the current meters.

RESULTS AND DISCUSSION

Hydrology

From the Θ-S°/₀₀ diagrams, the following different water masses which may be recognized are (see Fig. 3):

- Superficial and subsuperficial waters with high temperature and salinity (central water) to a depth of about 600 m.

- Antarctic intermediate water (AIW) (between about 600 m and 1 100 m). This water mass which is formed by sinking of Antarctic surface water at the Antarctic convergence, is characterized by a salinity minimum (about 34,7°/₀₀) which is situated in this area at a depth of about 750 m.

- Deep Atlantic water (between 1 100-1 200 m and about 4 000 m). It consists of a superposition of different deep waters formed in the North Atlantic, namely: Mediterranean water marked by a salinity maximum (about 35.00°/₀₀) at 1 600 m; Labrador Sea water; Norwegian Sea water.

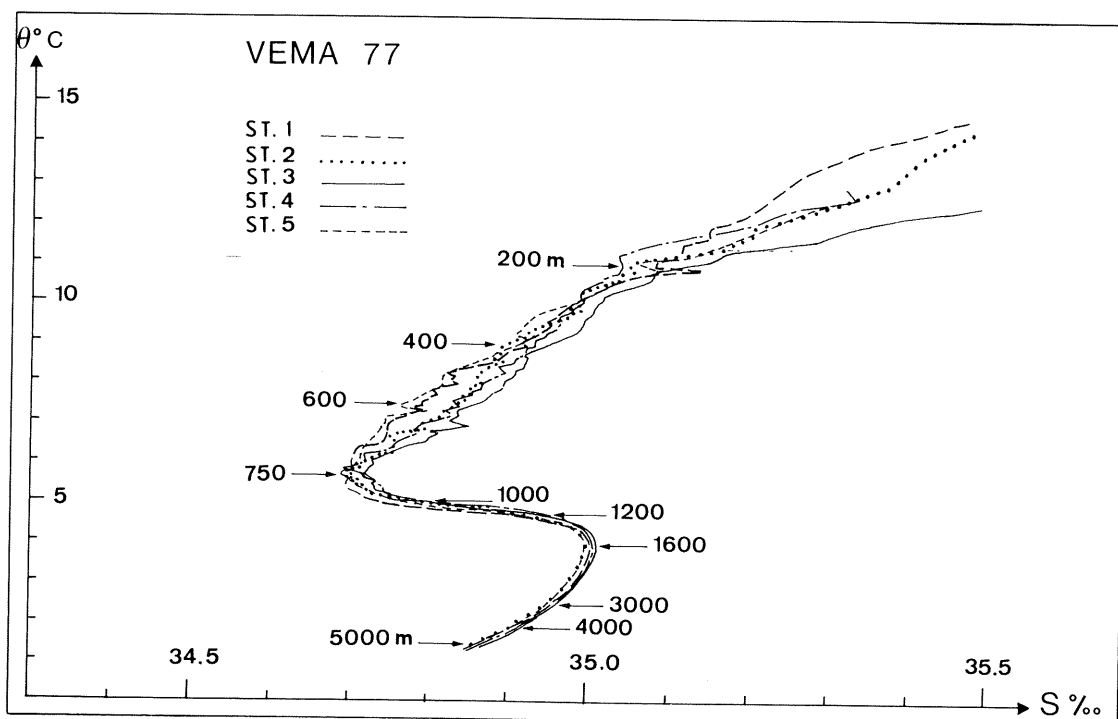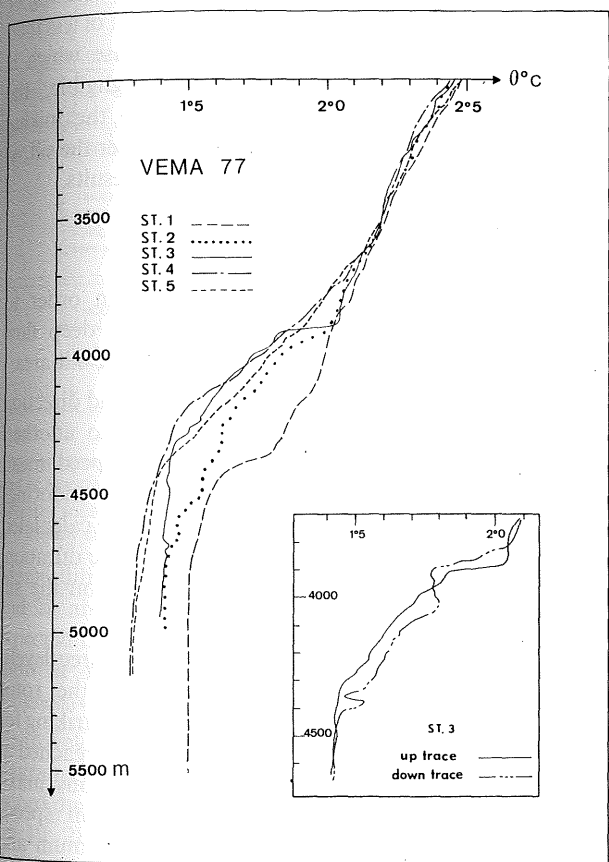The lower limit of this deep water mass which lies between 3 800 m and 4 000 m (except for station No 1), is

Figure 3

Θ S°/₀₀ diagrams for the five CTD profiles.
Diagrammes Θ-S°/₀₀ pour les cinq profils CTD.

well indicated by a step on the vertical profiles of temperature and salinity, the so-called "Benthic thermocline".

• Bottom water of Antarctic origin. This is an almost homogeneous water mass with low salinity (about 34.84‰) and low potential temperature (1.3 to 1.5°C in the area considered).

In order to study this bottom layer in greater detail, expanded deep potential temperature profiles have been drawn (see Fig. 4). All these profiles are those measured

Figure 4

Expanded deep potential temperature profiles, with detail for up and down-traces at station No. 3.

Profils profonds dilatés de température potentielle avec détail pour montée et descente à la station n° 3.

during the probe descent, except for station No. 3 where the ascent trace was choosen. The down-trace at station No. 3 presents two steps at 3 900 and 4 400 m, and the trace between these two depths does not exactly resemble either the up trace or that of the nearest stations; this structure is due more likely to a vertical transient event at the benthic thermocline level than to an advective phenomenon; it is therefore preferable to use the ascent trace, which does not present such an internal transient event.

These profiles show that the potential temperature in the bottom layer increases from the western stations (Nos. 5 and 4) towards the eastern station (No. 1). This increase is almost non-existent between stations 5 and 4, but is significant between station 4 and stations 3 and 2, situated on the sill (0.1°C); it is also significant between station No. 2 and station No. 1 (0.09°C). Such a progressive increase, linked to a higher increase in the eastern part due to the overflow above the sill, confirms that the Antarctic Bottom Water flow is in a west-east direction.

A longitudinal section of deep potential isotherms shows the deep hydrological structure along the valley (see Fig. 5). It may be noted that the benthic thermocline is found neither at the same depth nor with the same thickness at the different stations.

Examination of Figures 4 and 5 permits comparison of the structures at different stations, the results of which are summarized in Table 2. The two western profiles are almost identical (stations 5 and 4). The benthic thermocline begins at about 3 600 m at both stations, ending at 4 400 m at station 5 and at 4 200 m at station 4 (see Table 2), with a thickness of 800 and 600 m respectively. Below, the bottom water is not strictly homogenous: the potential temperatures at the top and bottom levels of the bottom layer are also presented in Table 2.

Figure 5

Potential temperature longitudinal section with CTD profiles: the location of the station is indicated by a vertical line, which also represents the 2°C isotherm for that station.

Coupe longitudinale de température potentielle avec les profils CTD: la position de la station est indiquée par une ligne verticale qui coupe ce profil de la station sur l'isotherme 2°C.
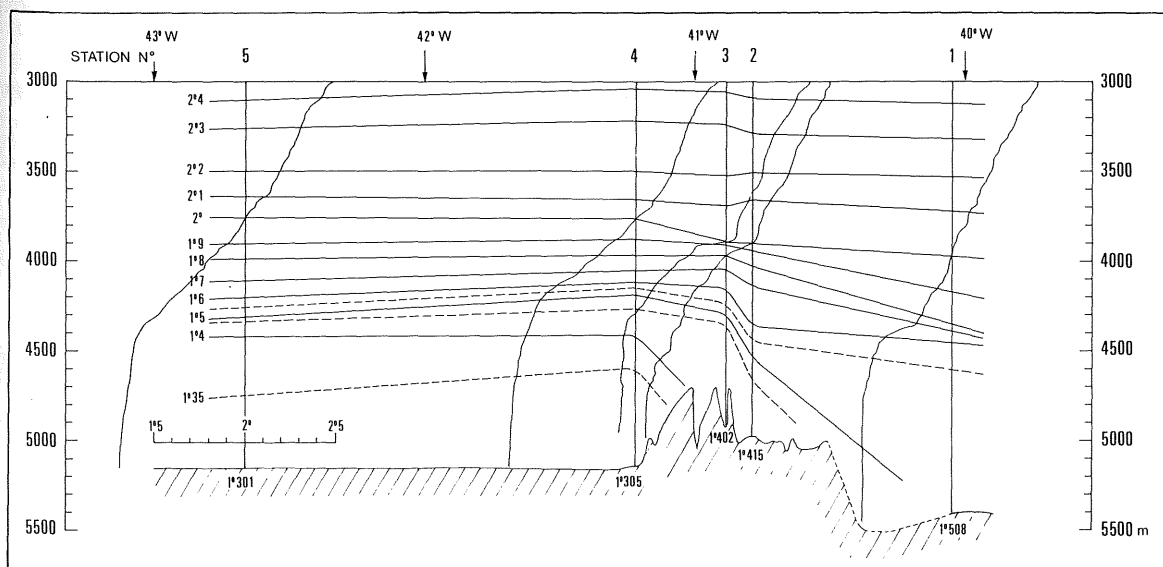
Table 2

Characteristics (potential temperatures and depths) of the benthic thermocline and of the bottom layer.
Caractéristiques (températures potentielles et profondeurs) de la thermocline benthique et de la couche de fond.

	Depth and Θ (°C) at the top of the thermocline		Thickness of the thermocline	Depth and Θ (°C) at the top of the bottom layer		Depth and Θ (°C) at the bottom		Thickness of the bottom layer
Station 1	4 350	1.80	100 m	4 450	1.61	5 452	1.508	1 000
Station 2	3 900	2.04	650 m	4 550	1.48	4 980	1.415	430
Station 3	3 900	2.05	400 m	4 300	1.46	4 944	1.402	650
Station 4	3 600	2.17	600 m	4 200	1.50	5.149	1.305	950
Station 5	3 600	2.15	800 m	4 400	1.41	5 166	1.301	750

The thickness of the bottom water layer is 750 and 950 m at stations 5 and 4 respectively. It may be observed that despite the considerable distance between these two stations (about 150 km), temperatures are almost identical at both.

On the contrary, east of the sill (station No. 1), we find a very homogeneous bottom water with a significant potential temperature increase (1.508°C at the bottom: 5 452 m). From 4 750 m down to 5 452 m (the bottom), the potential temperature is quite homogeneous (1.50°C). At this station, the benthic thermocline, which lies between 4 350 and 4 450 m, is deeper and thinner than that observed at stations 5 and 4.

Between these two configurations, stations 3 and 2 indicate an intermediate situation, with a less homogeneous bottom layer. At these two stations, the deepest level of the North Atlantic Deep water layer is found at about 3 900 m. Below this level, the benthic thermocline presents at first a strong step and then a smoother slope down to 4 300-4 500 m, where another step is found just before the bottom layer. This bottom layer is thinner than those of the other stations, and the potential temperature is not perfectly homogeneous (see Table 2).

On the longitudinal section (see Fig. 5), it may be seen that the benthic thermocline thins and deepens from west to east. The bottom layer is thinnest on the sill (stations 3 and 2) and most developed at the eastern station (station 1). On the sill, the profiles (3 and 2) are more affected by small temperature fluctuations than those of the western (Nos. 5 and 4) and eastern (No. 1) stations. This longitudinal section shows how the deep potential isotherms are deflected by the sill. Some of them are stopped by the sill itself, while the upper ones deepen just downstream of the sill. The thick, warmer homogeneous bottom layer at the eastern station (No. 1) is the product of an important stirring process linked with the intense turbulence which occurs above the sill. Both vertical and lateral mixing are responsible for these configurations.

An attempt to evaluate the possible effect of heat flow through the floor on the slight increase of bottom temperature was made with a computation similar to that employed by V. Fehn *et al.* (1977) for the Famous area. Heat flows were measured by M. G. Langseth and M. A. Hobart (1976). The used flow velocity was 10 cm/sec., which is a good average for the west-east mean flows measured at the different locations along the valley. This computation yields a maximum heating of bottom water between station 5 and station 1 of less than $1^\circ/_{00}$ of the measured temperature increase which is 0.207°C. Thus, this effect is quite negligible, the temperature increase being due solely to the mixing induced by the intensification of the flow over the sill, as illustrated by the current measurement results.

Currents

Current measurements were carried out in order to obtain quantitative results concerning the deep flow along the valley, and more specifically in the sill area.
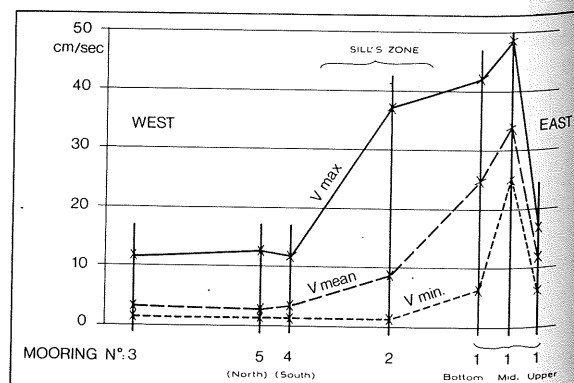
Significant differences as far as both speed and direction are concerned appear from one mooring to another. Figure 6 represents the values of maximum speed, mean speed and minimum speed for the different moorings and different levels. Averages and extremes are calculated from non-filtered data over all the record time duration. Speeds are higher eastward of the sill than on the sill itself and are very low west of the sill.

East of the sill, at mooring No. 1, at the three levels, minimum speeds are always larger than the rotor threshold value (1.5 cm/sec.), which is rather striking for such deep measurements. Highest values are reached at bottom and mid-levels, for both instantaneous maximum speeds (42 and 48 cm/sec.), and mean speeds (25 and 34 cm/sec.). At the upper level, maximum and mean speeds are 17 and 11 cm/sec. respectively. Such high values at this mooring, which were unexpected,

Figure 6

Schematic representation of minimum, mean and maximum speed values for the seven current meters records.
Representation schématique des valeurs minimum, moyennes et maximum des vitesses mesurées par les sept courantomètres.

are nevertheless consistent with the hydrological observations, which indicate increased mixing above the sill due to the intensification of the flow at this location. The speed record at the bottom level presents an important noise at frequencies higher than 1 cycle/hour (see Fig. 7) which appears also on mooring No. 2 speed and direction records. At these bottom levels, the order of magnitude of the noise is 1 $(cm/sec.)^2/c.$ p. h., while it is only 10^{-2} $(cm/sec.)^2/c.$ p. h. at mooring No. 4. This important noise may be related to the intense turbulence over the sill area.
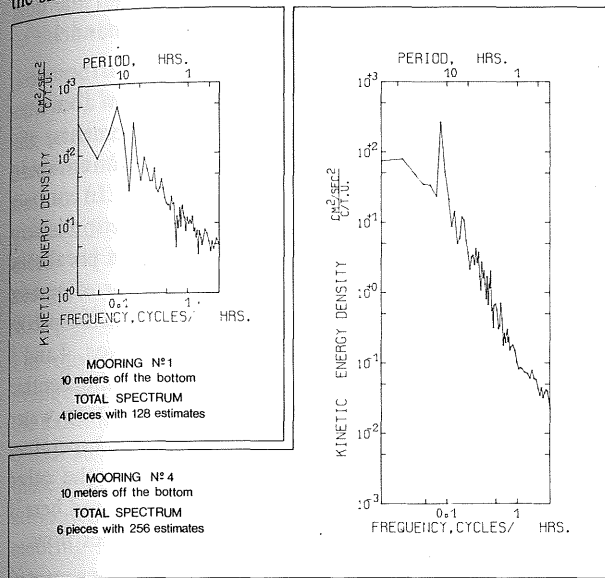

Figure 7

Total spectrum for two different records: at mooring No. 1, bottom level and at mooring No. 4.

Spectres totaux pour deux enregistrements différents : au mouillage n° 1 (fond) et au mouillage n° 4.

Mean directions for these four records (moorings 1 and 2) are in good agreement with the directions expected from hydrological and topographical data. All show a mean easterly or north-easterly flow (see progressive vector diagrams, Fig. 8).

Mean velocities are computed from progressive vector diagrams (PVD) as the mean daily trajectory over all the record duration. For mooring No. 1, the mean velocities are 10, 28 and 29 km/day for the upper, middle, and bottom levels respectively. Despite the different record durations, the consistency of speeds and directions permits comparison of these results (for the longest record, the mean velocity is the same over the short period when all instruments were working as throughout the entire record duration). Mean velocities are of the same order at the two deepest levels and are about three times lower at the upper zone.

At mooring No. 2, the mean velocity is only 2.5 km/day. Such a difference must be interpreted with care, because the current meter at mooring No. 2 was located on the bottom of a small depression, measuring 3 km in diameter, at a depth more than 200 m beneath the neighbouring intermediate sills (see Fig. 2). The main flow could be concentrated above the sill level. Considering the bathymetry, this location could explain the smaller measured speeds and the high current direction variability. The smaller mean velocity is a consequence of these two facts.
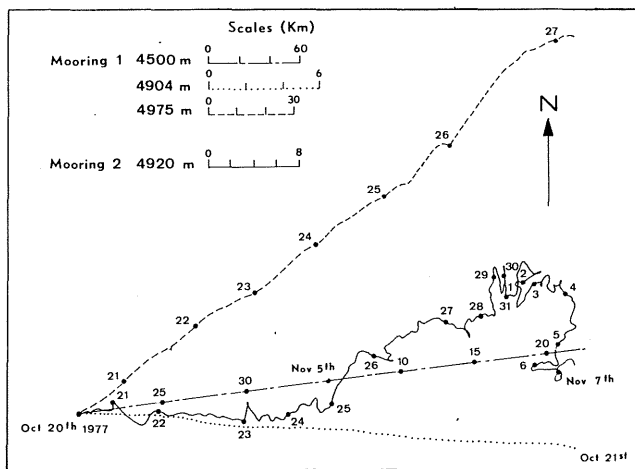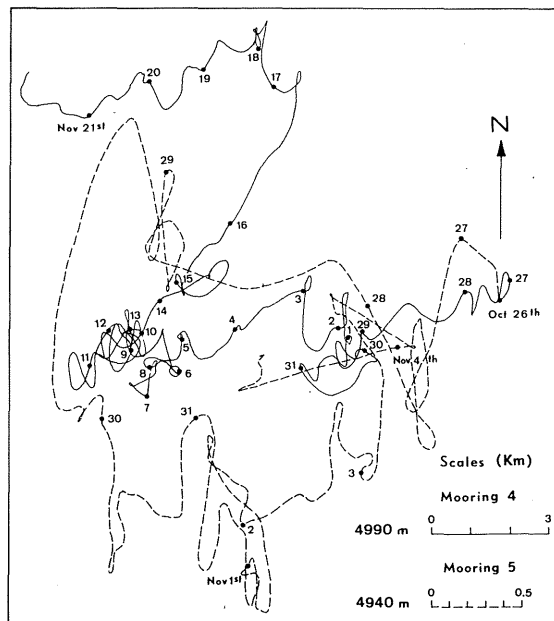

Figure 8

Progressive vector diagrams for moorings Nos. 1 and 2's current data.
Hodographes intégrés pour les données des mouillages n°s 1 et 2.

The perfect consistency of current direction at the upper level on mooring No. 1, is surprising. This cannot be due to compass failure because the instrumental tests made both before and after the cruise were satisfactory. Another technical explanation could be a direction error induced, at high pressure, by the nickel-coated container of the RCM 5 (Hendry, Hartling, 1979). But the consistency of the measured direction with those measured at the other levels leads us to believe that this feature is physically significant.

West of the sill, the flow is quite different. At moorings Nos. 4 and 5, maximum speeds are 12 cm/sec. and mean speeds are only 3.7 and 2.9 cm/sec. Minimum speeds are often less than the rotor threshold value, even during rather long periods of the records. Mean velocity is less than 1 km/day (0.6 and 0.35 km/day). No preferential flow direction appears during the record durations (8.5 and 26 days). The currents are dominated by semi-diurnal oscillations which are essentially north-south oriented (see Fig. 9), and which are not in phase at

Figure 9

Progressive vector diagrams for moorings Nos. 4 and 5's current data.
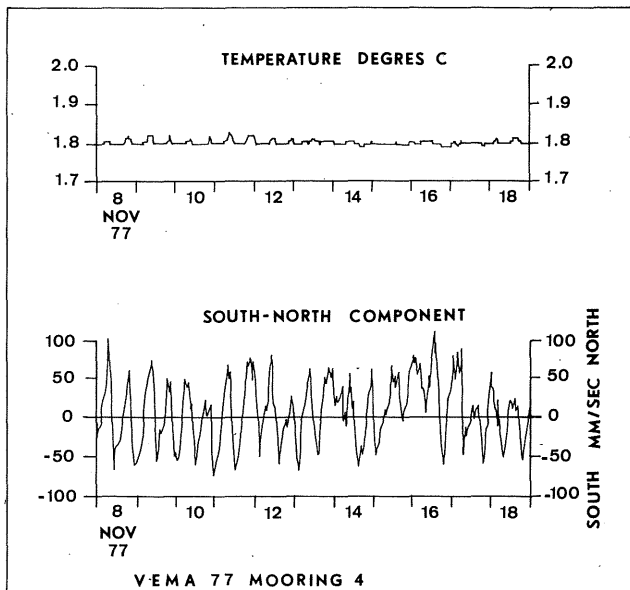Hodographes intégrés pour les données des mouillages n°s 4 et 5.

Figure 10

Temperature and North-South component of current recorded versus time at mooring No. 4.

Température et composante Nord-Sud du courant en fonction du temps pour le mouillage n° 4.

moorings Nos. 4 and 5. Over a distance of some 4 nautical miles, mooring No. 5 lags mooring No. 4 by about 1 hour which indicates a northward wave propagation speed of 4 knots. In this area, the external tide moves in this same direction, but much more quickly than the wave observed here. It may thus be deduced that the observed wave is an internal phenomenon which could be generated by the surface tide.

The temperature recorded by the current meter on the high resolution channel shows slight temperature oscillations (± 0.008°C) correlated with the north-south oscillation for moorings Nos. 4 and 5. At mooring No. 4 which is on the southern slope of the valley, the temperature increases at the end of the northward flow (see Fig. 10). At mooring No. 5 (on the northern flank), the temperature increases at the end of the southward flow. In both cases, temperatures begin to rise a few tens of minutes after the current has begun to flow towards the middle of the valley; this suggests that there is a vertical movement advecting warmer upper water when the current heads towards the valley bottom. These temperature fluctuations cannot be due to a depth oscillation of the mooring because, if this were the case, the temperature increase would occur not once but twice during the semi-diurnal period at each current reversal. Nor is the phenomenon due to a progressive internal wave, because in that case the temperature increase should appear with the same phase of the current oscillations at both moorings. The advection hypothesis is thus a better explanation for the observed temperature oscillation. The resulting isotherm oscillation comprises a deepening of isotherms near the northern flank of the valley when the current flows towards the south and a deepening of isotherms near the southern flank when the current flows toward the north.

The lack of data for the valley axis itself precludes any assertion concerning the flow in the middle of the valley,

but the currents measured on each side show that there is no counter-current just west of the sill as might have been supposed.
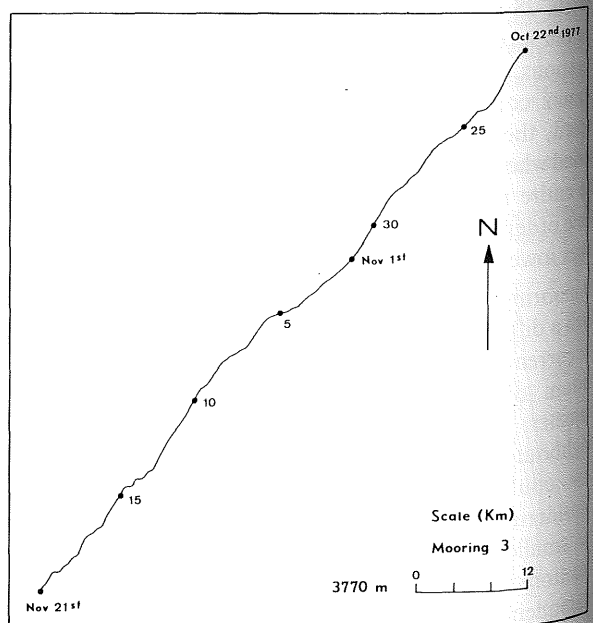
Current data records on and west of the sill reveal two different dynamic features: on the sill, the mean flow toward the east prevails, whereas west of the sill, the semi-diurnal north-south oscillation is predominant. Hydrological results indicate that the bottom temperature increase is more important on the sill than west of it. This means that the more important mixing process is the mean flow through the channel, rather than the tidal oscillation which is not aligned along the channel.

The fifth current meter, moored 200 km further west, was on the southern flank of the valley 230 m above the bottom. During the 30 days of measurements, the recorded current was very weak, with a maximum speed of 11 cm/sec. and a mean speed of 3.2 cm/sec. In contrast with conditions just west of the sill, the direction is very steady toward the southwest; this direction is parallel to the local isobaths (see progressive vector diagram, Fig. 11). Consequently, and despite similar mean speeds, the mean velocity is higher than at mooring Nos. 4 and 5 (2.66 km/day). The current meter was in the benthic thermocline and closer to North Atlantic Deep water than to bottom water. This explains why the temperature record presents higher oscillations than at the other moorings. The southwestward current measured here is consistent with the North Atlantic Deep water flow.

Because many of these records are too short, spectral analysis gives poor results. For the longest ones, the only significant peaks correspond to semi-diurnal and quarter-diurnal oscillations (see, for example, the mooring No. 4 spectrum in Figure 7). Spectral analysis and all current data processing were made in accordance with the WHOI (Woods Hole Oceanographic Institution) routine.

The bottom water volume transport through the passage was estimated by calculations based on the cross-section

Figure 11

Progressive vector diagram for mooring No. 3 current data.

Hodographe intégré pour les données du mouillage n° 3.

area of the trough and on the measured mean velocity at each measurement location on the sill area. Data from moorings Nos. 4 and 5 cannot be used, as they are on each side of the valley; not can data from mooring No. 3 be used, because the current meter was not exactly in the bottom layer.

For the moorings located on the sill area, the lack of bathymetric data for the northern part of the sill does not permit an exact estimate of the cross-section area available for bottom water transport. The depth of the isotherm $\Theta = 1.50°C$ is a good estimate for the upper level of the bottom water.

For mooring No. 1, the computed cross-section area was obtained by extrapolation of the bathymetric profile of the southern half. The volume transport computed on the basis of the mean velocity measured 10 m above the bottom (33 cm/sec.) amounts to $0.46 \times 10^6 m^3/sec.$; the volume transport computed with the mean velocity measured 300 m above the bottom (11 cm/sec.) would of course, be only a third of the previously stated value, i. e. $0.16 \times 10^6 m^3/sec.$

For mooring No. 2, an exact bathymetric profile is available. The only measured mean velocity 10 m above the bottom (2.8 cm/sec.) gives a volume transport of $0.05 \times 10^6 m^3/sec.$ This result is much lower than those obtained at mooring No. 1. The difference may be attributed either to the lesser speeds measured at mooring No. 2, or to an over estimation of the cross-section area at mooring No. 1 (or to both). These rough calculations give an order of magnitude for the volume transport, but supplementary current measurements at comparable levels, combined with a more complete bathymetric survey would be necessary to determine this volume with precision.

CONCLUSION

Hydrological measurements confirm the eastward flow of Antarctic Bottom water through the Vema Fracture Zone, and its overflow over the sill located in its eastern part.

Current measurements indicate that this flow is intensified over the sill area, where the currents reach a speed of almost one knot in a easterly or north-easterly direction. This result is consistent with the hydrological findings, which indicate that the progressive temperature increase of bottom water from west to east is more significant just on and beyond the sill, in association with the more important turbulence above the sill.

The bottom layer is quite homogeneous with a thickness of 750-950 m to the west of the sill. This layer is disturbed by the intense movements above the sill, which induce vertical and lateral stirring. Downstream of the sill, the eastern profile shows a thick (up to 1 000 m) homogeneous warmer bottom layer which is a product of the intense mixing above the sill. Bottom potential temperatures increase from 1.301°C half-way down the western valley to 1.402°C on the sill, and to 1.508°C beyond the sill.

West of the sill zone, current records on each side of the valley do indicate neither an eastward nor a return flow. On the contrary, speeds and current directions at this point are very unstable and are dominated by north-south oriented semi-diurnal oscillations. The semi-diurnal increase in temperature which appears at these two locations appears to be due to an advection phenomenon along the slope of the northern and southern flanks of the Fracture Zone valley.

REFERENCES

Eittreim S., Amos A. F., 1974. Bottom water characteristics of Vema Fracture Zone (abstract), *Eos*, (Am. Geophys. Union Trans.), **55**, 316 p.

Fehn U., Siegel M. D., Robinson G. R., Holland H. D., Williams D. L., Erickson A. J., Green K. E., 1977. Deep-water temperatures in the Famous area, *Geol. Soc. Am. Bull.*, **88**, 488-494.

Heezen B. C., Gerard R. D., Tharp M., 1964. The Vema Fracture Zone in the Equatoriel Atlantic, *J. Geophys. Res.*, **69**, 4, 733-739.

Hendry R. M., Hartling. A. J., 1979. A pressure induced direction error in nickel-coated Aanderaa current meters, *Deep-Sea-Res.*, **26**, No. 3 A, 327-354.

Langseth M. G., Hobart M. A., 1976. Interpretation of heat flow measurements in the Vema Fracture Zone, *Geophys. Res. Lett.*, **3**, 5, 241-244.

Renard V., Allenou J. P., 1979. Le Seabeam, sondeur à multi-faisceaux du N.O. "Jean Charcot". Description, évaluation et premiers résultats, *Rev. Hydrogr. Int. Monaco*, **LVI, 1**.

Van Andel Tj. H., Corliss J. B., Bowen V. T., 1967. The intersection between the Mid-Atlantic Ridge and the Vema Fracture Zone in the North Atlantic, *J. Mar. Res.*, **25**, 3, 343-351.

Van Andel Tj. H., Von Herzen R. P., Phillips J. D. , 1971. The Vema Fracture Zone and the tectonics of transverse shear zones in oceanic crustal plates, *Mar. Geophys. Res.*, **1**, 261-283,